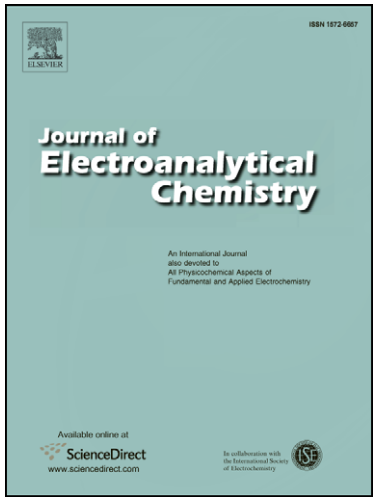

Evaluation of the structure-activity relationship of thrombin with thrombin binding aptamers by voltammetry and atomic force microscopy

Victor Constantin Diculescu, Ana-Maria Chiorcea-Paquim, Ramon Eritja, Ana Maria Oliveira-Brett

PII: S1572-6657(10)00501-1
DOI: 10.1016/j.jelechem.2010.11.037
Reference: JEAC 339

To appear in: *Journal of Electroanalytical Chemistry*

Received Date: 8 September 2010
Revised Date: 26 November 2010
Accepted Date: 29 November 2010

Please cite this article as: V.C. Diculescu, A-M. Chiorcea-Paquim, R. Eritja, A.M. Oliveira-Brett, Evaluation of the structure-activity relationship of thrombin with thrombin binding aptamers by voltammetry and atomic force microscopy, *Journal of Electroanalytical Chemistry* (2010), doi: 10.1016/j.jelechem.2010.11.037

Evaluation of the structure-activity relationship of thrombin with thrombin binding aptamers by voltammetry and atomic force microscopy

Victor Constantin Diculescu[1], *Ana-Maria Chiorcea-Paquim*[1], *Ramon Eritja*[2] *and Ana Maria Oliveira-Brett*[1*]

[1] Departamento de Quimica, Faculdade de Ciências e Tecnologia, Universidade de Coimbra, Portugal

[2] Institute for Research in Biomedicine, IQAC-CSIC, CIBER-BBN Networking Centre on Bioengineering, Biomaterials and Nanomedicine, Barcelona, Spain.

brett@ci.uc.pt

Ana Maria Oliveira-Brett

Departamento de Quíimica, Faculdade de Ciências e Tecnologia,

Universidade de Coimbra,

3004-535 Coimbra, Portugal

Abstract

The structure-activity relationship of the complex between thrombin and thrombin binding aptamers (TBA) was evaluated by differential pulse voltammetry at a glassy carbon electrode and atomic force microscopy at a highly oriented pyrolytic graphite electrode. The effects on the interaction with thrombin of TBA primary and secondary structures as well as of its folding properties in the presence of alkaline metals were investigated. The complex between thrombin and single stranded aptamers involved the coiling of the single stranded molecules around thrombin structure leading to the formation of a robust TBA-thrombin complex that maintains the symmetry and conformation of the thrombin molecule. Monitoring both thrombin and TBA oxidation peaks, showed that the thrombin oxidation peaks occur at more positive potentials after TBA-thrombin complex formation. In the presence of K^+ ions, the aptamers fold into quadruplex structures that facilitate the interaction with thrombin molecules. The TBA-thrombin complex adsorbs at the surface with the aptamer quadruplex always in preferential contact with the surface, and the thrombin molecules on top of the aptamer quadruplex structure, thus being less accessible to the electrode surface leading to the occurrence of thrombin oxidation peaks at less positive potentials.

Keyword: thrombin, aptamer, quadruplex, guanine, AFM, electrochemistry, oxidation.

1 Introduction

Thrombin is a serine protease and a coagulation protein in the blood stream that has many effects on the coagulation mechanism [1-3]. The activation of thrombin is a crucial process in physiological and pathological coagulation and various rare diseases involving thrombin have been described. For example, blood from a ruptured cerebral aneurysm clots around a cerebral artery and releases thrombin, which can induce an acute and prolonged narrowing of the blood vessel, potentially resulting in cerebral ischemia and infarction (stroke). In order to treat these diseases, potent and specific antithrombotic agents are required and their development continues to be an area of intensive research. These inhibitors must show the adaptation of natural inhibitors to the unique molecular architecture of thrombin [1].

Aptamers are DNA or RNA molecules that can be selected from random pools based on their ability to bind other molecules [4-7]. Aptamers have been selected to bind other nucleic acids, proteins, small organic compounds, and even entire organisms. They offer several advantages over antibodies, owing to their relative ease of isolation and modification, tailored binding affinity, and resistance to denaturizing [6]. Research focused on aptamers has exhibited promising potential in various fields such as pharmaceutics and diagnostics [8].

Aptamers with strong affinity for a wide range of protein targets have been identified [4-10]. One of the most intensely studied aptamers is the thrombin binding aptamer (TBA), the DNA 15-mer 5'-GGTTGGTGTGGTTGG-3' oligonucleotide that specifically binds to thrombin, inhibiting its activity [5, 11, 12]. It has been shown that TBA forms a unimolecular quadruplex in K^+ ion containing solution, arranged in a chair-like structure, consisting of two G-quartets connected by two TT loops and a

single TGT loop. It is this structure that has a great influence in the inhibition process of thrombin by TBA. However, the knowledge of the thrombin 3-dimensional structure also has a crucial importance in understanding this binding process.

A particularly striking feature of the thrombin molecule [13], Scheme 1, is its pronounced uneven charge distribution resulting in high positive and negative electrostatic field strengths outside the thrombin surface [2, 14]. In addition to the active site and the adjacent hydrophobic pocket (the apolar binding site), there are two electropositive exosites, the fibrinogen-recognition exosite at the base of the active-site cleft, and a more strongly electropositive heparin-binding exosite. It has been demonstrated that TBA does not interact with the active site of thrombin but with both exosites I and II [14, 15].

The detection and quantification of proteins play an essential role in fundamental research and clinical applications [16-19]. Different strategies for thrombin detection have been used and the combination of the perfect sensitivity and specificity of biologically active molecules with suitable transducers allowed the development of several types of biosensors [20-26]. Most of these biosensors involve complicated architectures and the detection of the binding processes is done through different mediators by optical and electrochemical transduction. Therefore, the characterization of the binding process between thrombin and TBA without any labelling emerges as a necessary step for the development and characterization of more sensitive detection devices. Moreover, the characterization of the thrombin-TBA complex is essential for the understanding of the factors involved in the binding process between thrombin and TBA.

The present paper is the first report of a systematic study to elucidate the mechanism of interaction of two different sequences, Scheme 2, thrombin binding aptamer (TBA, 5'-GGTTGGTGTGGTTGG-3') and extended thrombin binding aptamer (eTBA, 5'-GGGTTGGGTGTGGGTTGGG-3') [27, 28] with thrombin. The study was carried out on two different types of carbon electrode, glassy carbon using differential pulse voltammetry and highly oriented pyrolytic graphite using magnetic AC mode atomic force microscopy.

2 Experimental

2.1 Materials and reagents

Thrombin from Human Plasma obtained from Sigma-Aldrich was used without further purification. The ODN sequences TBA and eTBA, were synthesized on an ABI 3400 DNA Synthesizer (Applied Biosystems, Foster City, CA, USA) using the 200-nmol scale synthesis cycle [27]. All solutions were prepared using analytical grade reagents and purified water from a Millipore Milli-Q system (conductivity ≤ 0.1 μS cm^{-1}). Stock thrombin, TBA and eTBA solutions were prepared in Milli Q water and kept at 4 ºC. Before each experiment, solutions of thrombin, TBA or eTBA were freshly prepared by dilution of the appropriate quantity in pH 7.0 0.1 M phosphate buffer (0.2 M Na_2HPO_4 + 0.2 M NaH_2PO_4). The designation for the single stranded aptamers of ss-TBA and ss-eTBA and for the quadruplex aptamers of qs-TBA and qs-eTBA will be used.

Microvolumes were measured using EP-10 and EP-100 Plus Motorized Microliter Pippettes (Rainin Instrument Co. Inc., Woburn, USA). The pH measurements

were carried out with a Crison micropH 2001 pH-meter with an Ingold combined glass electrode. All experiments were done at room temperature (25 ± 1 ºC).

2.2 Atomic force microscopy

The substrate used in magnetic AC mode atomic force microscopy (MAC mode AFM) study was highly oriented pyrolytic graphite (HOPG), grade ZYB of dimensions 15 x 15 x 2 mm^3, from Advanced Ceramics Co., USA. The HOPG was freshly cleaved with adhesive tape prior to each experiment and imaged by AFM in order to establish its cleanliness.

AFM was performed in the AAC mode AFM, with a PicoScan controller from Agilent Technologies, Tempe, AZ, USA. All the AFM experiments were performed with a CS AFM S scanner with a scan range of 6 μm in *x*-*y* and 2 μm in *z*, from Agilent Technologies. AppNano type FORT of 225 μm length, 3.0 N m^{-1} spring constants and 47 – 76 kHz resonant frequencies in air (Applied NanoStructures, Inc., USA) were used. All AFM images were topographical and were taken with 256 samples/line x 256 lines and scan rates of 0.8 – 2.0 lines s^{-1}. When necessary, the AFM images were processed by flattening in order to remove the background slope and the contrast and brightness were adjusted.

2.3 Sample preparation for AFM

TBA–thrombin and eTBA–thrombin solutions were prepared by incubation at room temperature of 1 μg mL^{-1} TBA or eTBA with 0.25 μg mL^{-1} or 10 μg mL^{-1} of thrombin in pH 7.0 0.1 M phosphate buffer. To study the influence of the K^+ ions, the

incubation of the TBA-thrombin and eTBA-thrombin solutions was performed in the presence of 100 mM KCl.

The thrombin, TBA, eTBA, TBA–thrombin and eTBA–thrombin modified HOPG surfaces were obtained by depositing 200 µL samples of the appropriate solution of thrombin, TBA, eTBA, TBA–thrombin or eTBA–thrombin solutions onto the freshly cleaved HOPG surface, during 5 min. The excess of solution was gently removed by cleaning with a jet of Millipore Milli-Q water, and the HOPG with adsorbed molecules was then dried in a sterile atmosphere and imaged by AAC Mode AFM in air.

2.4 Voltammetric parameters and electrochemical cells

Voltammetric experiments were carried out using a µAutolab running with GPES 4.9 software, Metrohm/Autolab, Utrecht, The Netherlands. Measurements were carried out using a glassy carbon (GCE, d = 1.5 mm) working electrode, a Pt wire counter electrode, and a Ag/AgCl as reference, in a 0.25 mL electrochemical cell. The experimental conditions for differential (DP) voltammetry were pulse amplitude 50 mV, pulse width 70 ms, and scan rate 5 mV s^{-1}.

The GC electrode was polished using diamond spray (particle size 1 µm) before each experiment. After polishing, the electrode was rinsed thoroughly with Milli-Q water and placed in supporting electrolyte and various DP voltammograms were recorded until a steady state baseline voltammogram was obtained. This procedure ensured very reproducible experimental results.

All results have been repeated several times with good reproducibility. It must be mentioned that each measurement was always done using a freshly polished GCE, a process that give rise to small modifications of the electrode surface area which can in

turn cause variations in the current, however lower than 5 % and this is the main source of differences in the currents in the procedures described.

2.6 Sample preparation for voltammetry

TBA-thrombin and eTBA-thrombin solutions were prepared by incubation at room temperature of 1 μg mL^{-1} TBA/eTBA with 1 μg mL^{-1} of thrombin in pH 7.0 0.1 M phosphate buffer.

To study the influence of the K^+ ion concentration, two different experiments were carried out. In the first, the incubation of the TBA-thrombin and eTBA-thrombin solutions was performed in the presence of 100 mM KCl. In the second, TBA or eTBA were incubated during 24 h with 100 mM KCl in order to obtain the formation of the quadruplexes and than incubated with thrombin.

2.5 Acquisition and presentation of voltammetric data

The DP voltammograms were baseline-corrected using the moving average with a step window of 2 mV included in GPES version 4.9 software. This mathematical treatment improves the visualization and identification of peaks over the baseline without introducing any artefact, although the peak height is in some cases reduced (<10%) relative to that of the untreated curve. Nevertheless, this mathematical treatment of the original voltammograms was used in the presentation of all experimental voltammograms for a better and clearer identification of the peaks. The values for peak current presented in all plots were determined from the original untreated voltammograms after subtraction of the baseline.

3 Results

3.1 Adsorption process and redox behaviour of thrombin

3.1.1 AFM characterization of adsorbed thrombin

The capacity of thrombin to interact and adsorb on carbon electrode surfaces was investigated using AFM in air. The thrombin modified HOPG was obtained by spontaneous adsorption during 5 min, from solutions of either 0.25 or 10 μg mL^{-1} thrombin, using the method described in *Section 2.3*.

AFM images of the thrombin modified HOPG obtained from a solution of 0.25 μg mL^{-1} thrombin in pH 7.0 0.1 M phosphate buffer, showed the formation of aggregates of 2.0 – 4.0 of height, presenting the tendency to attach near the defects on the HOPG step edges, **Fig. 1A**. Increasing the concentration of thrombin to 10 μg mL^{-1}, a large number of aggregates clusters could be observed in the images, **Fig. 1B and C**, presenting heights of 3.9 ± 0.6 nm.

Since a greater adsorption of thrombin was observed for 10 μg mL^{-1} concentrated solutions allowing a better visualization on the AFM images, all experiments were carried out in these conditions.

3.1.2 Voltammetric characterization of thrombin, TBA and eTBA

DP voltammograms were recorded with the clean GCE in solutions of thrombin of different concentrations in pH 7.0 0.1 M phosphate buffer. Two consecutive peaks, T_1 at E_{pa}^{1} = + 0.76 V, and T_2 at E_{pa}^{2} = + 0.90 V, **Fig. 1D**, were always observed at the same potentials with currents varying proportionally to the concentration.

DP voltammograms in pH 7.0 0.1 M phosphate buffer in solutions of 1 μg mL^{-1} ss-TBA and ss-eTBA showed a main oxidation peak G at E_{pa}^{G} = + 0.88 mV, due to the oxidation of guanine residues [28]. This peak presented higher currents in the case of eTBA, in agreement with a greater number of guanine residues when compared with TBA. Upon formation of the quadruplexes (qs), the DP voltammograms showed a smaller peak G for both aptamers. Nevertheless, in the case of qs-eTBA a new peak G_q occurred at more positive potentials and this peak, previously characterized, is specific to the G-quadruplex oxidation [28].

DP voltammograms were also obtained with different concentrations of thrombin incubated with solutions of 1 μg mL^{-1} TBA or eTBA. Higher peaks and a better separation of the electrochemical signals of thrombin, TBA or eTBA, were observed for concentrations of 1 μg mL^{-1} thrombin and so all further experiments were carried out in these conditions.

3.2 Interaction of thrombin binding aptamers with the thrombin

3.2.1 AFM evaluation of TBA–thrombin and eTBA–thrombin interaction

The mechanism of interaction with thrombin of both thrombin binding aptamers, TBA and eTBA, was investigated and characterized by AFM. The TBA–thrombin or eTBA–thrombin modified HOPG surfaces were obtained as described in *Section 2.3*, by spontaneous adsorption from incubated solutions of 1 μg mL^{-1} TBA or eTBA with 10 μg mL^{-1} thrombin in pH 7.0 0.1 M phosphate buffer, during several periods of time. This procedure led to co-adsorption of TBA or eTBA–thrombin, free TBA or eTBA and free thrombin molecules.

The stabilisation of the quadruplex structures requires the presence of metal ions, in particular alkali metals, and the order of preference is $K^+ > Na^+$. Both buffer solutions used in this study contain only Na^+, although acetate buffer contains a lower Na^+ concentration than the phosphate buffer solution. In order to establish the influence of the presence of K^+ in the formation and stabilisation of TBA and eTBA quadruplexes, modifying their interaction with thrombin, the morphological characteristics of TBA–thrombin or eTBA–thrombin modified HOPG surfaces obtained from solutions of TBA–thrombin and eTBA–thrombin incubated in the presence of 100 mM KCl during different periods of time, were also analysed.

AFM images of the ss-TBA-thrombin modified HOPG, obtained after adsorption from pH 7.0 0.1 M phosphate buffer, 1 μg mL^{-1} TBA and 10 μg mL^{-1} thrombin solutions without incubation, showed almost complete HOPG surface coverage by a network film of 0.9 ± 0.1 nm height, with embedded 2.3 ± 0.4 nm height spherical aggregates. After 24 h of incubation, **Fig. 2A**, the height of the network was 1.0 ± 0.3 nm and of the aggregates 2.5 ± 0.1 nm.

A more complicated situation was observed for qs-TBA-thrombin formed after the addition of K^+ ions and incubation during 24 h, **Fig. 2B**. The HOPG surface coverage decreased drastically and patches of a thick layer with bulky, knotty appearance were observed due to the existence of a large number of aggregates embedded into its structure. The heights of the layer were very heterogeneous, between 1.0 and 3.6 nm.

The interaction between thrombin and eTBA was also evaluated by AFM. The AFM images of the ss-eTBA-thrombin modified HOPG obtained after adsorption from pH 7.0 0.1 M phosphate buffer, 1 μg mL^{-1} eTBA and 10 μg mL^{-1} thrombin

solutions incubated during 1 h, **Fig. 3A**, showed the HOPG surface covered by an incomplete ss-eTBA–thrombin but thick network, with knotty appearance and 2.3 ± 0.5 nm height. After 24 h of incubation in the presence of only Na^+ cations, **Fig. 3B**, the AFM images showed the formation of the thick, 2.9 ± 0.7 nm height areas that were previously observed after short incubation times.

AFM images of the qs-eTBA–thrombin modified HOPG, obtained after adsorption from pH 7.0 0.1 M phosphate buffer, 1 μg mL^{-1} qs-eTBA and 10 μg mL^{-1} thrombin solutions in the presence of 100 mM K^+, showed a mixed pattern of adsorption after both 1 h, **Fig. 3C**, and 24 h, **Fig. 3D**, of incubation with 2.9 ± 0.3 nm thickness and 3.4 ± 0.4 nm height.

3.2.2 Voltammetric evaluation of TBA–thrombin and eTBA–thrombin interaction

The interaction of thrombin and TBA was investigated after incubation of 1 μg mL^{-1} thrombin with 1 μg mL^{-1} TBA in pH 7.0 0.1 M phosphate buffer. The DP voltammograms were recorded after different incubation periods and between experiments the GCE surface was always cleaned in order to avoid poisoning of the electrode surface with TBA and/or thrombin oxidation products formed after successive voltammograms in solution.

The DP voltammograms recorded immediately after the addition of 1 μg mL^{-1} ss-TBA to the solution of 1 μg mL^{-1} thrombin in pH 7.0, **Fig. 2C**, showed the two peaks of thrombin, T_1 and T_2, and the oxidation peak G of ss-TBA. No differences in the potential and current when compared with the voltammograms in the solution containing only thrombin or TBA were observed. Increasing the incubation times, both thrombin oxidation peaks, T_1 and T_2, occurred with the same current but at a higher

potential, ΔE_p ~ 20 mV. Additionally, peak G was not observed. An increase of the peak at E_p ~ + 0.90 V was observed in the DP voltammograms after different incubation times due to the overlapping of ss-TBA oxidation peak G and of thrombin oxidation peak T_2. Nevertheless, thrombin peak T_1 occurred always with the same current.

The same experiments were carried out in a mixed solution of 1 μg mL^{-1} thrombin and 1 μg mL^{-1} qs-TBA in pH 7.0. The DP voltammograms obtained without incubation, **Fig. 2D**, showed the occurrence of the thrombin oxidation peak T_1 at the same potential and with the same current as the voltammograms recorded in the solution containing only thrombin. The increase in the current at E_p ~ +0.90 V, due to the overlapping of qs-TBA oxidation peak G and of thrombin oxidation peak T_2 was observed. It is important to mention that upon formation of qs-TBA, peak G decreased drastically; hence it cannot be observed on this voltammograms. Increasing the incubation time, both peaks decreased in a time-dependent manner during 48 h of incubation after which constant currents were reached, **Fig. 5**.

The interaction of thrombin with ss-eTBA was studied after incubation of 1 μg mL^{-1} thrombin with 1 μg mL^{-1} eTBA in pH 7.0 0.1 M phosphate buffer. The DP voltammograms were recorded after different incubation periods and between experiments the GCE surface was always cleaned. The DP voltammograms recorded immediately after addition of 1 μg mL^{-1} eTBA to the solution of 1 μg mL^{-1} thrombin in pH 7.0, **Fig. 4A**, showed thrombin and eTBA oxidation peaks at the same potential and with the same current as in the voltammograms in the solution containing only thrombin or eTBA. A small increase of the thrombin oxidation potential of peaks, T_1 and T_2, ΔE_p ~ 20 mV, was observed in the voltammograms recorded after different incubation periods. The peak at E_p ~ + 0.90 V showed an increase in current since it was due to

both thrombin peak T_2 and peak G of eTBA. Nevertheless, thrombin peak T_1 occurred always with the same current and potential.

A different situation was observed when the experiments were carried out in a mixed solution of 1 μg mL^{-1} thrombin and 1 μg mL^{-1} qs-eTBA in pH 7.0. On the DP voltammograms recorded immediately after addition of qs-eTBA to the solution of thrombin, **Fig. 4B**, a new peak G_q due to the oxidation of eTBA quadruplexes was observed. On the other hand, thrombin peak T_1 occurred with the same current as the voltammograms recorded in the solution containing only thrombin, while the peak at E_p ~ + 0.90 V was due to the overlapping of peaks T_2 and G. The voltammograms obtained after different incubation times showed a gradual decrease of thrombin oxidation peak $T_1$and of the peak at E_p ~ + 0.90 V. Nevertheless, peak G_q occurred always with the same current. The changes that occurred for both thrombin oxidation peaks were followed during 168 h incubation, **Fig. 5**. A faster decrease of thrombin oxidation currents was observed in the first 48 h of incubation, **Fig. 5**, but for longer times constant currents were reached.

4 Discussion

Protein adsorption is a complex phenomenon and both the biological activity and amount of adsorbed proteins depend on the properties of the substrate. Although the complex interactions between solid surfaces and proteins are not completely understood, it is believed that both short and long range forces including van der Waals interactions, electrostatic interactions, hydrogen bonding and particularly hydrophobic interactions are all very important in protein adsorption [21]. The thrombin molecule has only small hydrophobic moieties which are the active-site and the apolar binding

site (the adjacent hydrophobic pocket). For this reason, a small adsorption of thrombin at the HOPG surface was observed, **Fig. 1 A-C**. However, the voltammetric results showed that the thrombin molecule is oxidised presenting two peaks corresponding to its electroactive centres, **Fig. 1D**.

In a previous report [28] it has been shown that, in the presence of K^+ cations, due to the formation of very stable and rigid intramolecular quadruplex configurations, both TBA and eTBA adsorb less onto HOPG, compared to their adsorption in the presence of only Na^+ cations, as in the pH 7.0 0.1M phosphate buffer. This is due to the fact that a larger number of intramolecular quadruplexes is formed, which are more stable due to the incorporation of K^+, which prevents the aptamers hydrophobic interaction with HOPG. The presence of only Na^+ cations led to the formation of less stable quadruplexes [29] that are locally destabilised by the HOPG hydrophobic surface, inducing the aptamers' greater adsorption together with the single-stranded sequences [28]. The voltammetric studies showed that both TBA and eTBA are oxidized at GCE and the only electrochemical signal is due to the oxidation of guanine residues, peak G. Upon addition of K^+ ions, both TBA and eTBA fold into G-quadruplex structures, Scheme 2, and this process was observed by the decrease of the peak G and the occurrence of a new peak G_q at higher potential values due to the oxidation of guanine residues in the G-quartets [28].

In the present study, the AFM and the voltammetric results for the interaction of thrombin with different structures of TBA and eTBA were evaluated.

The AFM images obtained after the incubation of thrombin with ss-TBA or ss-eTBA showed the formation of a network film with embedded aggregates that almost completely covered the HOPG surface, **Table 1 and Figs. 2A, 3A and 3B**. This film

involves the co-adsorption of ssTBA–thrombin or ss-eTBA–thrombin, free ss-TBA or ss-eTBA and free thrombin molecules. Increasing the incubation time, the height of both network and aggregates increased and this process is specific to the formation of the ssTBA-thrombin complex.

The voltammetric results showed that, by increasing the incubation time, the peak currents of both thrombin oxidation peaks, T_1 and T_2, remain constant, but their potentials become more positive **Figs. 2C and 4A**, while peak G occurs at the same potential. This causes overlapping of the peaks T_2 and G which explains the increase of the current observed at + 0.90 V on the DP voltammograms for longer incubation times. The increase in potential of peaks T_1 and T_2 may be explained considering the formation of ss-TBA-thrombin or ss-eTBA-thrombin complexes that do not involve either of thrombin exocites but the coiling of the single stranded molecules around parts of the thrombin structure. This interaction is most probably electrostatic and occurs between the negatively charged phosphate backbone of the aptamers and positive electrostatic field strength outside the thrombin surface leading to the formation of a robust complex as was also shown by the AFM images. Therefore, the transition of electrons from the inside of the rigid aptamer-thrombin complex to the GCE surface is more difficult than from the more flexible thrombin molecule that can reach the surface more easily leading to higher peak currents.

A complicated situation was observed after the incubation of thrombin with qs-TBA or qs-eTBA. The AFM images showed patches of a thick layer with a bulky, knotty appearance due to the existence of a large number of embedded aggregates into its structure, **Figs. 2B, 3C and 3D**. The heights of the layer were very heterogeneous, varying between 1.0 and 3.6 nm, **Table 1**. The decrease of adsorption when compared

with the interaction between ss-TBA or ss-eTBA and thrombin is explained by a reduced number of single stranded oligonucleotides that may adsorb at the HOPG surface. On the other hand, considering that qs-TBA or qs-eTBA can interact with either both or any of the thrombin exocites, this layer may be due to the adsorption of at least three types of aggregates dictated by the interaction with either one or both thrombin exocites.

In agreement with the AFM results, the voltammetric studies have shown that, increasing the incubation time, the decrease of both thrombin oxidation peaks T_1 and T_2 occurs, **Figs. 2D and 4B**. This effect is specific to conformational changes in biological molecules, but the occurrence of structural modification of thrombin upon binding of qs-TBA or qs-eTBA is improbable considering previous studies [30]. On the other hand, it has been shown that the G_q peak remains constant, maintaining the same current even for long incubation times, suggesting that upon incubation the qs-TBA or qs-eTBA are always in contact with the electrode surface. The thrombin molecules lie on top of the aptamer quadruplex structure: the reduced contact between thrombin molecules and the GCE surface leads to the occurrence of lower oxidation peak, T_1 and T_2, currents.

In order to study the influence of the K^+ ions on the TBA or eTBA interaction with thrombin, two different voltammetric experiments were carried out. In one experiment TBA or eTBA were incubated during 24 h with 100 mM KCl, in order to form the quadruplexes, and afterwards incubated with thrombin, as described above. In the other experiment the incubation of the TBA-thrombin and eTBA-thrombin solutions was performed in the presence of 100 mM KCl in order that the formation of the aptamer quadruplex occurred in the presence of thrombin. Nevertheless, similar results were obtained in both cases.

4 Conclusion

A systematic study of the interaction between thrombin and two different thrombin binding aptamer sequences was carried out on two different types of carbon electrode, GCE using DP voltammetry and HOPG using MAC mode AFM.

The AFM results obtained after the incubation of thrombin with single stranded aptamers showed for low incubation times the co-adsorption of aptamer–thrombin, free aptamer and free thrombin molecules. Increasing the incubation time, the height of the aggregates increased in agreement with the formation of the aptamer-thrombin complex. The voltammetric results confirm these data and show that thrombin oxidation peaks occur at more positive potentials upon complex formation. This behaviour is explained considering coiling of the single stranded aptamer molecules around the thrombin structure leading to the formation of a more robust complex that maintains the conformation of the thrombin molecules.

After incubation of thrombin with quadruplex aptamers a complicated situation was observed. The AFM images showed patches of a thick layer with a bulky, knotty appearance due to the existence of a large number of embedded aggregates into its structure corresponding to the adsorption of different types of aggregates dictated by the interaction with either one or both thrombin exocites. The voltammetric data suggested that upon interaction with thrombin, the quadruplexes are always in contact with the electrode surface whereas the thrombin molecules lie above the quadruplex structure which reduces their contact with the electrode surface leading to the occurrence of lower thrombin oxidation peaks.

Acknowledgment

Financial support from Fundação para a Ciência e Tecnologia (FCT), Post-Doctoral Grant SFRH/BPD/36110/2007 (V.C. Diculescu), projects PTDC/QUI/65255/2006, PTDC/QUI/098562/2008 and PTDC/SAU-BEB/104643/2008, POCI 2010 (co-financed by the European Community Fund FEDER), and CEMUC-R (Research Unit 285), and COST Action MP0802 (Self-assembled guanosine structures for molecular electronic devices (G4-net) is gratefully acknowledged.

References

1 M.T. Stubbs, W. Bode, The clot thickens: clues provided by thrombin structure, Trends Biochem. Sci., 20 (1995) 23-28.

2 W. Bode, Structure and interaction modes of thrombin, Blood Cell. Mol. Dis., 36 (2006) 122–130.

3 W. Bode, I. Mayr, U. Baumann, R. Huber, S.R.Stone1, J. Hofsteenge, The refined 1.9 A° crystal structure of human α-thrombin: interaction with D-Phe-Pro-Arg chloromethylketone and significance of the Tyr-Pro-Pro-Trp insertion segment, EMBO J., 8 (1989) 3467-3475.

4 W. James, Aptamers, in Encyclopedia of Analytical Chemistry, ed. R.A. Meyers, 2000, pp. 4848–4871.

5 S. Chandra, B. Gopinath, Anti-coagulant aptamers, Thromb. Res., 122 (2008) 838–847.

6 H. Yang, J. Ji, Y. Liu, J. Kong, B. Liu, An aptamer-based biosensor for sensitive thrombin detection, Electrochem. Commun., 11 (2009) 38–40.

7 B. Prieto-Simon, M. Campas, J.-L. Marty, Electrochemical aptamer-based sensors, Bional. Rev., 1 (2009) 141-157.

8 S. Tombelli, M. Minunni, M. Mascini, Analytical applications of aptamers, Biosen. Bioelec., 20 (2005) 2424–2434.

9 Y. Liu, C. Lin, H. Li, H. Yan, Aptamer-Directed Self-Assembly of Protein Arrays on a DNA Nanostructure, Angew. Chem. Int. Ed., 44 (2005) 4333 –4338.

10 Y. Fang, Label-free receptor assays, Drug Discov. Today: Technologies, In Press, Corrected Proof, Available online 1 June 2010.

11 J. A. Kelly, J. Feigon, and T. O. Yeates, Reconciliation of the X-ray and NMR structures of the thrombin-binding aptamer d(GGTTGGTGTGGTTGG), J. Mol. Biol., 256 (1996) 417-422.

12 B. Pagano, L. Martino, A. Randazzo, C. Giancola, Stability and Binding Properties of a Modified Thrombin Binding Aptamer, Biophys. J., 94 (2008) 562–569.

13 J.L. Moreland, A.Gramada, O.V. Buzko, Q. Zhang, P.E. Bourne, The Molecular Biology Toolkit (mbt): A Modular Platform for Developing Molecular Visualization Applications. BMC Bioinformatics, 6 (2005) 21.

14 P. Jayapal, G. Mayer, A. Heckel, F. Wennmohs, Structure–activity relationships of a caged thrombin binding DNA aptamer: Insight gained from molecular dynamics simulation studies, J. Struct. Biol., 166 (2009) 241–250.

15 L.R. Paborsky, S.N. McCurdy, L.C. Griffin, J.J. Toole, L.LK. Leung, The Single-stranded DNA Aptamer-binding Site of Human Thrombin, J. Biol. Chem., 268 (1993) 20808-20811.

16 A. Vallée-Bélisle, K.W. Plaxco, Structure-switching biosensors: inspired by Nature, Curr. Opin. Struct. Biol., 20 (2010) 518-526.

17 T. Hianik, V. Ostatna, Z. Zajacova, E. Stoikova, G. Evtugyn, Detection of aptamer–protein interactions using QCM and electrochemical indicator methods, Bioorg. Med. Chem. Lett., 15 (2005) 291–295.

18 E. Baldrich, A. Restrepo, C.K. O'Sullivan, Aptasensor Development: Elucidation of Critical Parameters for Optimal Aptamer Performance, Anal. Chem., 76 (2004) 7053-7063.

19 B. Basnar, R. Elnathan, I. Willner, Following Aptamer-Thrombin Binding by Force Measurements, Anal. Chem., 78 (2006) 3638-3642.

20 M. Mir, M. Vreeke, I. Katakis, Different strategies to develop an electrochemical thrombin aptasensor, Electrochem. Commun., 8 (2006) 505-511.

21 P. Soman, Z. Rice, C.A. Siedlecki, Immunological identification of fibrinogen in dual-component protein films by AFM imaging, Micron, 39 (2008) 832–842.

22 H. Hasegawa, K. Taira, K. Sode, K. Ikebukuro, Improvement of Aptamer Affinity by Dimerization, Sensors, 8 (2008) 1090-1098.

23 C. Polonschii, S. David, S. Tombelli, M. Mascini, M. Gheorghiu, A novel low-cost and easy to develop functionalization platform. Case study: Aptamer-based detection of thrombin by surface plasmon resonance, Talanta, 80 (2010) 2157–2164.

24 A.-E. Radi, J.L.A. Sanchez, E. Baldrich, C.K. O'Sullivan, Reusable Impedimetric Aptasensor, Anal. Chem., 77 (2005) 6320-6323.

25 A.-E. Radi, J.L.A. Sanchez, E. Baldrich, C.K. O'Sullivan, Reagentless, Reusable, Ultrasensitive Electrochemical Molecular Beacon Aptasensor, J. Am. Chem. Soc., 128 (2006) 117-124.

26 R. Polsky, R. Gill, L. Kaganovsky, I. Willner, Nucleic acid-functionalized Pt nanoparticles: catalytic labels for the amplified electrochemical detection of biomolecules, Anal. Chem., 78 (2006) 2268-2271.

27 M. del Toro, R. Gargallo, R. Eritja, and J. Jaumot, Study of the interaction between the G-quadruplex-forming thrombin binding aptamer and the porphyrin 5,10,15,20-tetrakis-(Nmethyl-4-pyridyl)-21,23H-porphyrin tetratosylate, Anal. Biochem., 379 (2008) 8-15.

28 V.C. Diculescu, A.-M. Chiorcea-Paquim, R. Eritja, A.M. Oliveira-Brett, Thrombin-Binding Aptamer Quadruplex Formation: AFM and Voltammetric Characterization, Journal of Nucleic Acids, 2010 (2010) 1-8.

29 B.I. Kankia,L.A. Marky, Folding of the Thrombin Aptamer into a G-Quadruplex with Sr^{2+}: Stability, Heat, and Hydration, J. Am. Chem. Soc., 123 (2001) 10799-10804.

30 A. Virno, A. Randazzo, C. Giancola, M. Bucci, G. Cirino, L. Mayol, A novel thrombin binding aptamer containing a G-LNA residue, Bioorgan. Med. Chem., 15 (2007) 5710–5718.

Table 1 – Thrombine, TBA, eTBA, TBA–thrombine and eTBA–thrombine modified HOPG morphological characteristics by AFM.

Solution in pH 7.0 0.1 M phosphate buffer		**Adsorption pattern and heights**	**Time**	**Figure**
10 μg mL^{-1} thrombin	-	3.9 ± 0.6 nm aggregates clusters		1C
1 μg mL^{-1} TBA	-	0.8 ± 0.1 nm network/fragments (ss-TBA) 1.9 ± 0.5 nm aggregates (qs-TBA)		[27]
	+ 100 mM K^+	0.8 ± 0.1 nm network/fragments (ss-TBA)		[27]
1 μg mL^{-1} TBA + 10 μg mL^{-1} thrombin	-	0.9 ± 0.1 nm network 2.3 ± 0.4 nm aggregates	1 h	not shown
		1.0 ± 0.3 nm network 2.5 ± 0.1 nm aggregates	24 h	2A
	+ 100 mM K^+	1.0–3.6 nm thick, bulky, knotty film	24 h	2B
1 μg mL^{-1} eTBA	-	0.8 ± 0.1 nm network/fragments (ss-eTBA) 1.5 ± 0.5 nm aggregates (qs-eTBAs)	1 h	[27]
	+ 100 mM K^+	0.8 ± 0.1 nm network/fragments (ss-eTBA) few 1.5 ± 0.5 nm aggregates (qs-TBAs)	24	[27]
1 μg mL^{-1} eTBA + 10 μg mL^{-1} thrombin	-	2.3 ± 0.5 nm thick film	1 h	4A
		2.9 ± 0.7 nm thick, bulky, knotty film	24 h	4B
	+ 100 mM K^+	2.9 ± 0.7 nm thick, bulky, knotty film	1 h	4C
		3.4 ± 0.4 nm thick, bulky, knotty film	24 h	4D

Figures

Scheme 1 - Representations of the tertiary structure of thrombin generated by PDB Protein Workshop 3.8 (Powered by MBT) [13]. **(A)** Two main peptide chains are observed. Chain A at the top of the molecule and the heavier chain B below. **(B)** Representation of thrombin exocites I and II [2].

Scheme 2 - Schematic representation of anti-parallel quadruplex structures of **(A)** TBA and **(B)** eTBA.

Figure 1 - AFM topographical images in air of a thrombin modified HOPG surface, obtained by spontaneous adsorption during 5 min, from solutions of **(A)** 0.25 and **(B, C)** 10 μg mL^{-1} thrombin in pH 7.0 0.1 M phosphate buffer. **(D)** DP voltammograms base line corrected obtained with the GCE in solution of (▬) 0.25, (▪▪▪) 0.50 and (•••) 1.00 μg mL^{-1} thrombin in pH 7.0 0.1 M phosphate.

Figure 2 - AFM topographical images in air of a TBA–thrombin modified HOPG, obtained by spontaneous adsorption during 5 min from incubated solutions in pH 7.0 0.1 M phosphate buffer of 1 μg mL^{-1} TBA with 10 μg mL^{-1} thrombin, **(A)** in the absence and **(B)** in the presence of 100 mM K^+, after 24 h of incubation. **(C, D)** DP voltammograms base line corrected obtained with the GCE in incubated solutions of 1 μg mL^{-1} thrombin incubated with 1 μg mL^{-1}

(C) ss-TBA and **(D)** qs-TBA in pH 7.0 0.1 M phosphate buffer during (•••) 0, (—) 1 and (—) 48 h.

Figure 3 - AFM topographical images in air of eTBA–thrombin, immobilised on the HOPG surface by spontaneous adsorption during 5 min, from an incubated solution of 10 μg mL^{-1} thrombine with 1 μg mL^{-1} eTBA in pH 7.0 0.1 M phosphate buffer, **(A, B)** in the absence and **(C, D**) in the presence of 100 mM K^+, after **(A, C)** 1 h and **(B, D)** 24 h of incubation.

Figure 4 - DP voltammograms base line corrected obtained with the GCE in incubated solutions of 1 μg mL^{-1} thrombin with 1 μg mL^{-1} **(A)** ss-eTBA and **(B)** qs-eTBA in pH 7.0 0.1 M phosphate buffer during (•••) 0, (—) 1 and (—) 48 h.

Figure 5 - Plot of the variation with incubation time of thrombin oxidation peaks (●, ○) T_1 and (■, □) T_2 after incubation with 1 μg mL^{-1} (○,□) qs-TBA and (●,■) qs-eTBA.

Scheme 1 - Representations of the tertiary structure of thrombin generated by PDB Protein Workshop 3.8 (Powered by MBT) [13]. **(A)** Two main peptide chains are observed. Chain A at the top of the molecule and the heavier chain B below. **(B)** Representation of thrombin exocites I and II [2].

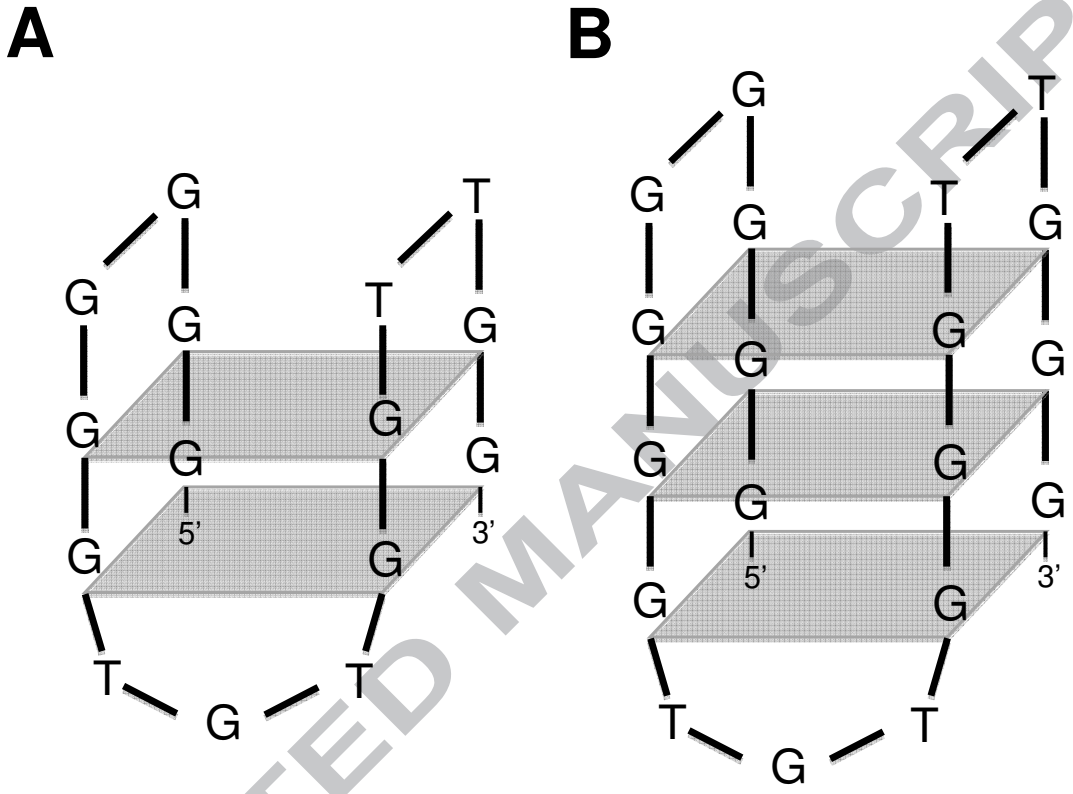

Scheme 2 - Schematic representation of anti-parallel quadruplex structures of **(A)** TBA and **(B)** eTBA.

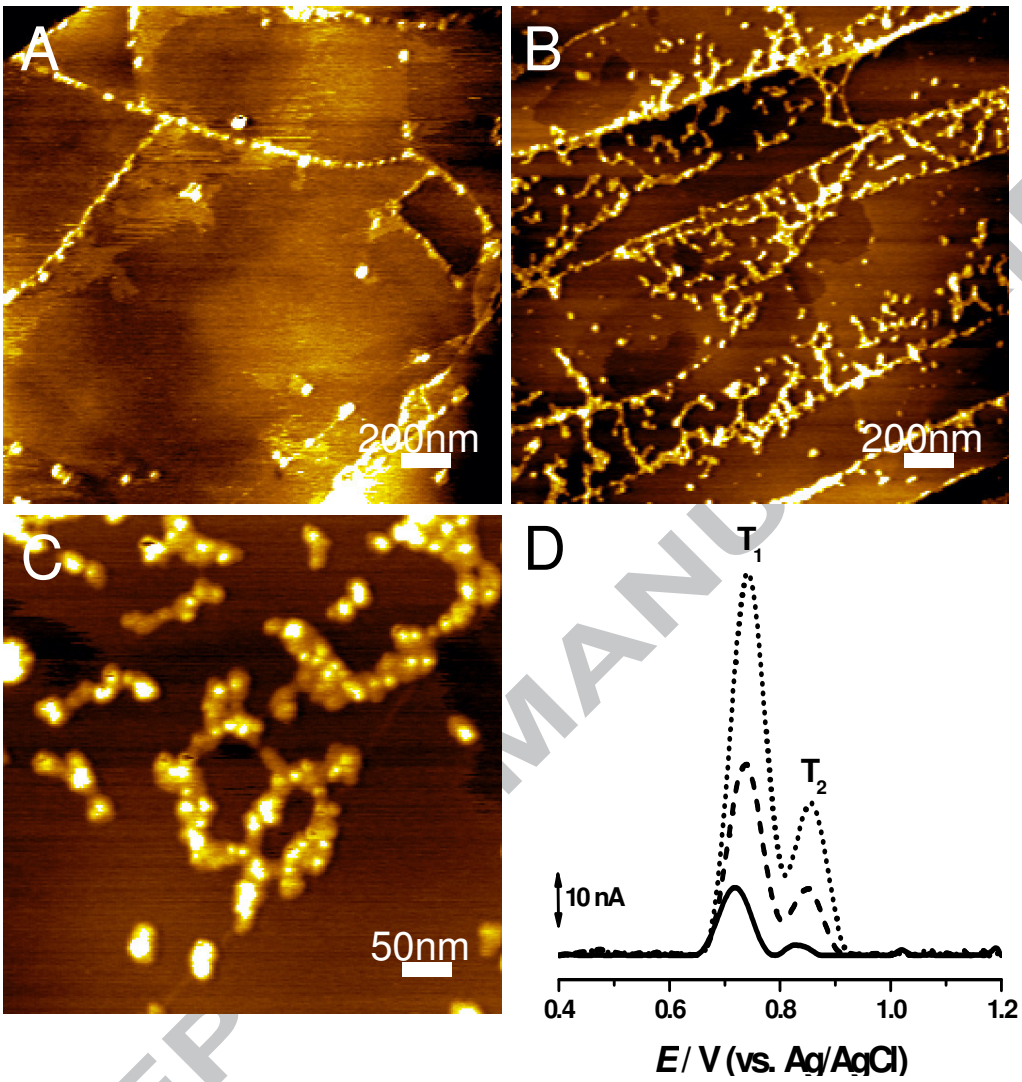

Figure 1 - AFM topographical images in air of a thrombin modified HOPG surface, obtained by spontaneous adsorption during 5 min, from solutions of **(A)** 0.25 and **(B, C)** 10 μg mL^{-1} thrombin in pH 7.0 0.1 M phosphate buffer. **(D)** DP voltammograms base line corrected obtained with the GCE in solution of (—) 0.25, (▪▪▪) 0.50 and (•••) 1.00 μg mL^{-1} thrombin in pH 7.0 0.1 M phosphate.

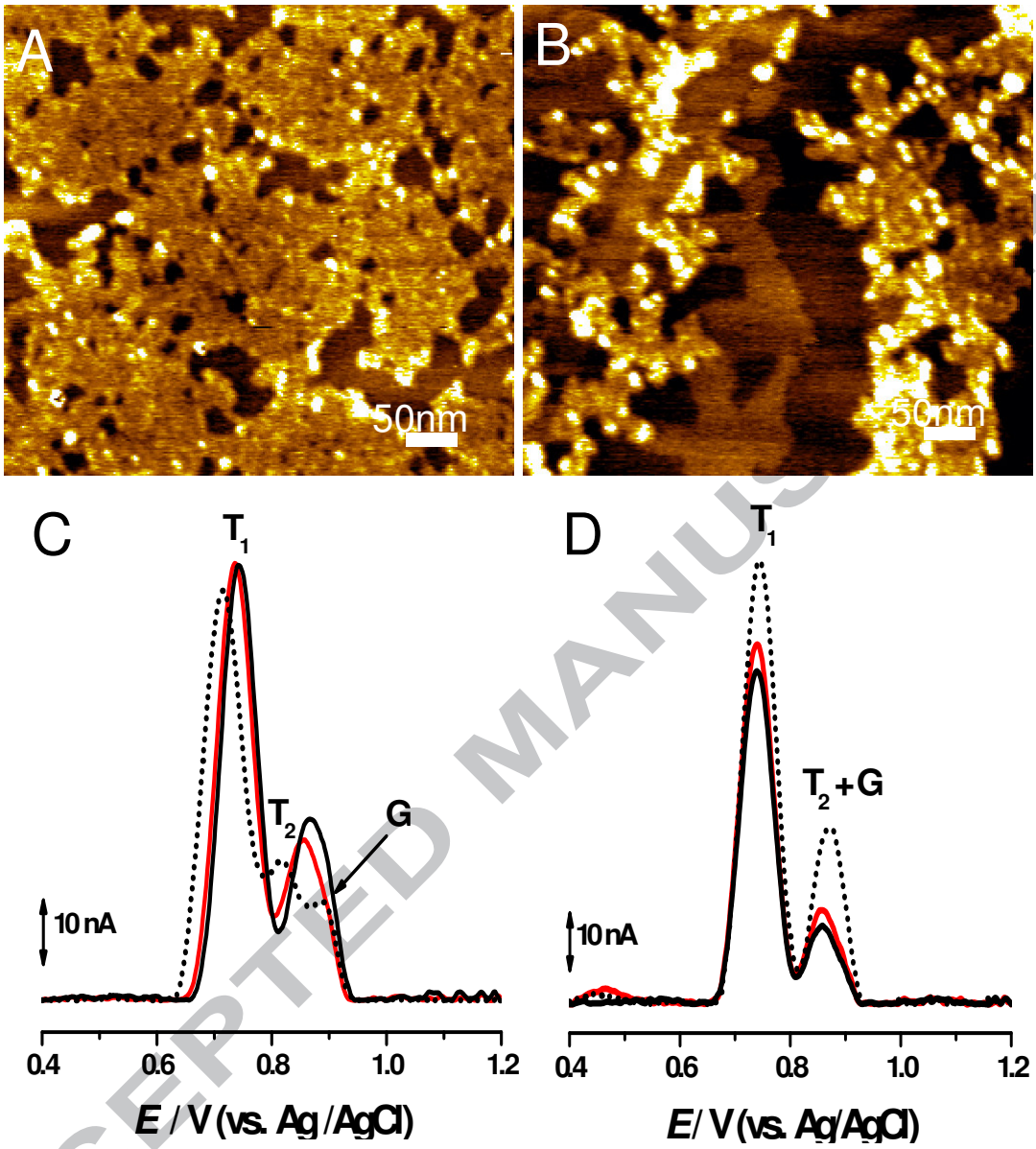

Figure 2 - AFM topographical images in air of a TBA–thrombin modified HOPG, obtained by spontaneous adsorption during 5 min from incubated solutions in pH 7.0 0.1 M phosphate buffer of 1 μg mL^{-1} TBA with 10 μg mL^{-1} thrombin, **(A)** in the absence and **(B)** in the presence of 100 mM K^+, after 24 h of incubation. **(C, D)** DP voltammograms base line corrected obtained with the GCE in incubated solutions of 1 μg mL^{-1} thrombin incubated with 1 μg mL^{-1} **(C)** ss-TBA and **(D)** qs-TBA in pH 7.0 0.1 M phosphate buffer during (•••) 0, (—) 1 and (—) 48 h.

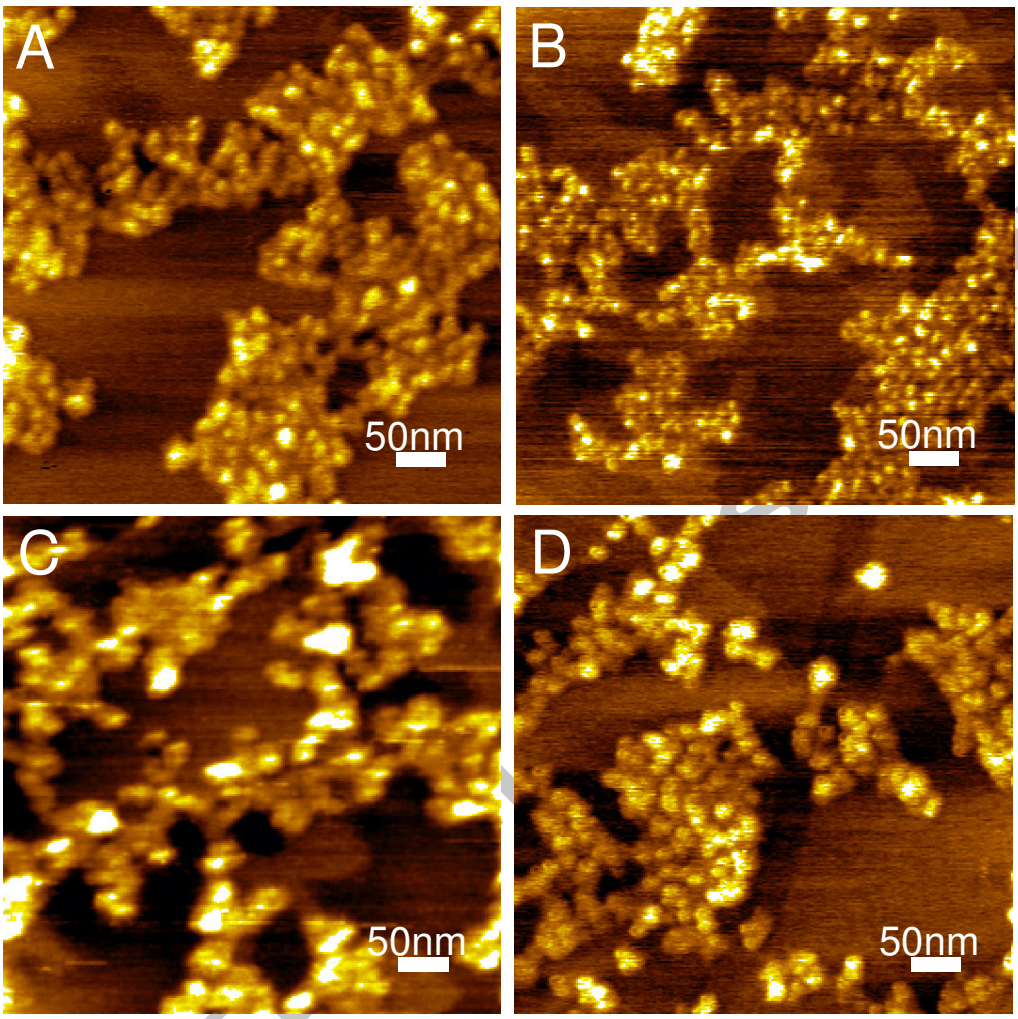

Figure 3 - AFM topographical images in air of eTBA–thrombin, immobilised on the HOPG surface by spontaneous adsorption during 5 min, from an incubated solution of 10 µg mL^{-1} thrombine with 1 µg mL^{-1} eTBA in pH 7.0 0.1 M phosphate buffer, **(A, B)** in the absence and **(C, D)** in the presence of 100 mM K^+, after **(A, C)** 1 h and **(B, D)** 24 h of incubation.

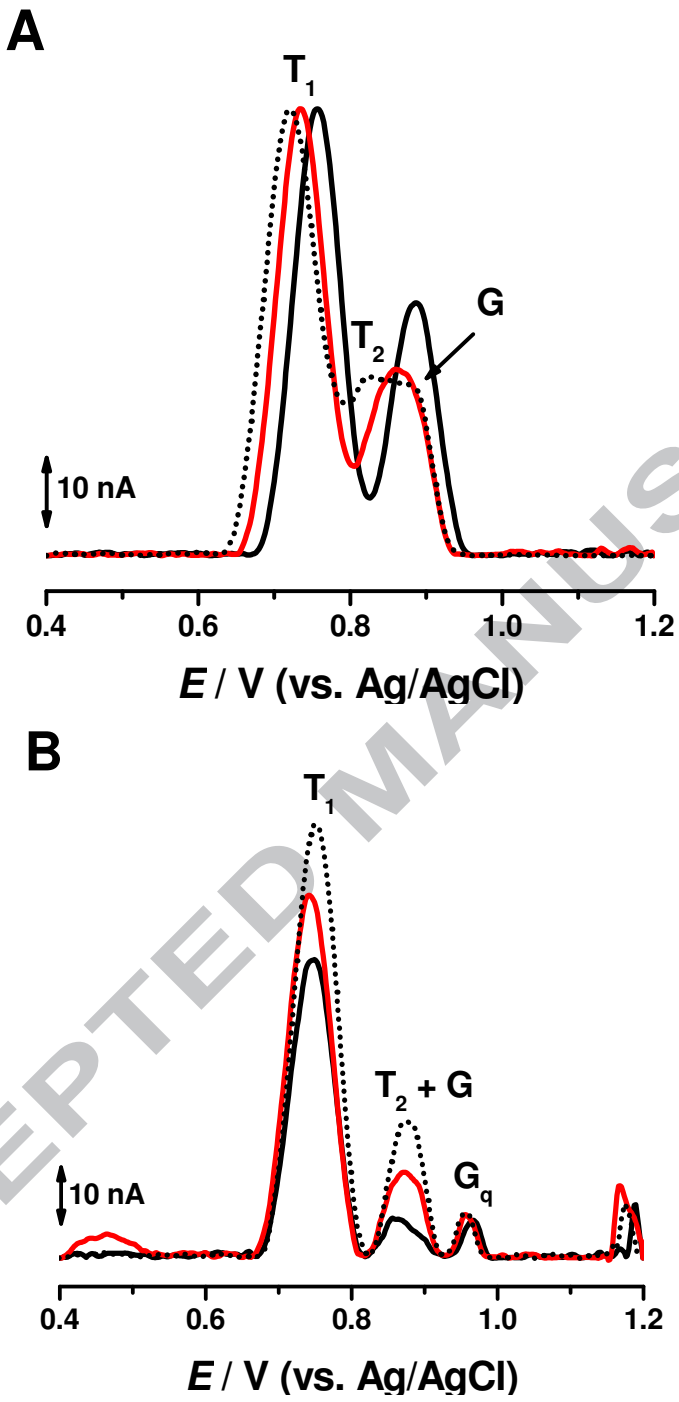

Figure 4 - DP voltammograms base line corrected obtained with the GCE in incubated solutions of 1 μg mL^{-1} thrombin with 1 μg mL^{-1} **(A)** ss-eTBA and **(B)** qs-eTBA in pH 7.0 0.1 M phosphate buffer during (•••) 0, (—) 1 and (—) 48 h.

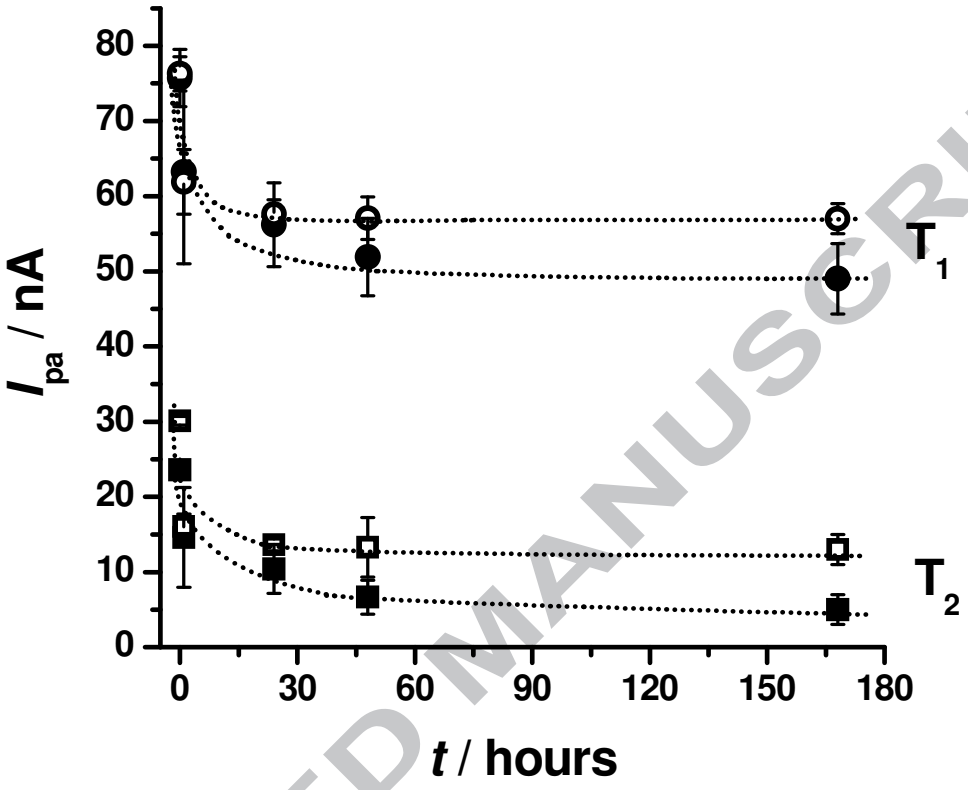

Figure 5 -Plot of the variation with incubation time of thrombin oxidation peaks (●, ○) T_1 and (■, □) T_2 after incubation with 1 μg mL^{-1} (○,□) qs-TBA and (●,■) qs-eTBA.